HHS Public Access

Author manuscript

ACS Appl Mater Interfaces. Author manuscript; available in PMC 2024 August 10.

Covalently Attached Slippery Surface Coatings to Reduce Protein Adsorptions on Poly(dimethylsiloxane) Planar Surfaces and 3D Microfluidic Channels

Yue Cao[1,†], **Xingchi Chen**[2,†], **Avi Matarasso**[3], **Zizheng Wang**[4], **Yang Song**[1], **Guangfu Wu**[1], **Xincheng Zhang**[1], **He Sun**[1], **Xueju Wang**[4], **Michael R. Bruchas**[3,5,6,7], **Yan Li**[2,*], **Yi Zhang**[1,*]

[1]Department of Biomedical Engineering and the Institute of Materials Science, University of Connecticut, Storrs, CT 06269, USA.

[2]Department of Chemical and Biomedical Engineering, FAMU-FSU College of Engineering, Florida State University, Tallahassee, FL 32306, USA.

[3]Department of Bioengineering, University of Washington, Seattle, WA 98195, USA

[4]Department of Materials Science and Engineering and the Institute of Materials Science, University of Connecticut, Storrs, CT 06269, USA.

[5]Department of Anesthesiology and Pain Medicine, University of Washington, Seattle, WA 98195, USA

[6]Center for Neurobiology of Addiction, Pain, and Emotion, University of Washington, Seattle, WA 98195, USA

[7]Department of Pharmacology, University of Washington, Seattle, WA 98195, USA

Abstract

Silicone elastomers, such as Poly (dimethylsiloxane) (PDMS), have a broad range of applications in basic biomedical research and clinical medicine, ranging from the preparation of microfluidic devices for organs-on-chips and ventriculoperitoneal shunts for the treatment of hydrocephalus to implantable neural probes for neuropharmacology. Despite the importance, the protein adsorptions on silicone elastomers in these application environments represent a significant challenge. Surface

[*]Corresponding author. yi.5.zhang@uconn.edu or yli@eng.famu.fsu.edu.
[†]These authors contribute equally.

Competing financial interests: The authors declare that they have no competing interests.

Data and materials availability: All data needed to evaluate the conclusions in the paper are present in the paper and/or the Supplementary Materials.

Supporting information

Table S1. Advantages and limitations of various surface coatings; Table S2. Quantitative fluorescence intensity analysis of planar PDMS surfaces with and without the slippery coating; Table S3. Quantitative fluorescence intensity analysis of 3D microfluidic channels with and without the slippery coating; Figure S1. X-ray photoelectron spectroscopy (XPS) spectra of the slippery surface coating on PDMS; Figure S2. The effects of active chemical solutions and treatments on the wetting properties of PDMS surfaces; Figure S3. The speed-dependent friction coefficients under a constant load force of 1 N for PDMS surfaces with and without the slippery surface coating; Figure S4. Anti-protein adsorption property of planar PDMS surfaces without coating and with the coating after mechanical treatments; Figure S5. Quantitative analysis of average fluorescence intensity of protein removal as a function of time for microfluidic channels with and without the surface coating; Movie S1. The mobility of water droplets on PDMS surfaces with the slippery coating at a tilt angle of 15°; Movie S2. The mobility of water droplets on bare PDMS surfaces at a tilt angle of 15°.

coatings with slippery lubricants, inspired by the *Nepenthes* pitcher plants, have recently received much attention for reducing protein adsorptions. Nevertheless, the depletion of the physically infused lubricants limits their broad applications. In this study, we report a covalently attached slippery surface coating to reduce protein adsorptions on PDMS surfaces. As demonstrations, we show that the adsorption of serum proteins, human fibrinogen and albumin, can be significantly reduced by the slippery surface coating on planar PDMS surfaces and in 3D microfluidic channels. The preparation of slippery surface coatings relies on acid-catalyzed polycondensation reaction of dimethyldimethoxysilane, which utilizes low-cost and scalable dip-coating method. Furthermore, cell metabolic activity and viability studies demonstrate the biocompatibility of the surface coating. These results suggest the potential applications of slippery surface coatings to reduce protein adsorptions for implantable medical devices, organs-on-chips, and many others.

Keywords

slippery surface coatings; PDMS; planar surfaces; 3D microfluidic channels; protein adsorptions

INTRODUCTION

Silicone elastomers, such as poly(dimethylsiloxane) (PDMS), have been widely used in the preparation of many clinically approved medical devices,[1] including breast implants,[2] dialysis membrane,[3] intraocular lens,[4, 5] and many others. Due to their material biocompatibility, tissue-like mechanical property (~ 1 MPa), and optical transparency, they are also frequently used in the emerging field of bioelectronics and biosensors, such as in microfluidics for tissue engineering,[6] wearable electronics for sweat samplings,[7-9] and implantable neural probes for neuropharmacology and neurochemical sampling.[10-12] Despite these attractive properties of PDMS-based materials and their wide range of applications, the non-specific protein adsorptions and resulting biofouling represent a significant challenge for these applications. For example, the protein adsorptions and immune response could block the microchannels of implantable microfluidics for drug delivery,[10-12] resulting in the device failure and replacement. Similarly, the protein adsorption on the PDMS encapsulation layers of implantable optogenetic devices could reduce the output intensity of the microscale light-emitting diodes (μ-ILEDs). Additionally, for implantable neural probes that are coated with PDMS layers, the damage of brain neurovascular during the probe implantation often causes the release of pro-inflammatory and neurotoxic serum proteins, such as fibrinogen and albumin, into the surrounding brain tissues.[13] These released proteins adsorb on the PDMS surface and promote the adhesion of microglia, thereby triggering a series of inflammatory immune responses and the formation of glial scars on the implant surfaces. These formed scars can encapsulate the implant surface and cause recording/stimulation performance degradation over time.[14]

To solve this issue, various surface coatings have been developed to minimize the protein adsorption and biofouling at material's surfaces (Table S1),[15, 16] including PDMS. Polyethylene glycol (PEG) and its derivatives are the gold-standard protein-resistant surface coatings for implantable devices.[17] Nevertheless, the PEG gel suffers from hydrolysis and oxidative degradation and enzymatic cleavage during *in vivo* applications.[18, 19]

Recently, zwitterionic polymers have been demonstrated to have exceptional anti-biofouling properties,[20-22] though they still face reduced stability in long-term operations due to the presence of the hydrolysis ester group.[23]

Slippery liquid-infused porous surfaces (SLIPS), inspired by the *Nepenthes* pitcher plants, have recently received much attention for various biomedical applications.[24-27] A recent study shows that a lubricant-infused neural probe significantly reduces the insertion damage and foreign body response.[28] Nevertheless, the lubricant depletion during the insertion represents a significant challenge due to the physically infused lubricant layer (lack of covalent bonding).[29-31] The lubricant depletion issue could be resolved by covalently grafting 'liquid-like' polymer brushes on the surface. Wu et al. reported a slippery 'liquid-like' surface for antibiofouling applications via water-assisted equilibration reactions of methoxy-terminated polydimethylsiloxane (PDMS-OCH_3).[32] Nevertheless, the relatively high temperature (120 °C) and lengthy preparation time (24 hours) could cause damage to the underlying bioelectronics, thereby limiting its broader applications. Different from the thermally activated reactions, the 'liquid-like' polymer brushes can be prepared by acid-catalyzed polycondensation reaction of dimethyldimethoxysilane,[33] which is time-efficient and can be operated at room temperatures. Nonetheless, there have not been any studies to report whether this surface coating can be used to reduce protein adsorptions on planar PDMS surfaces and 3D microfluidic channels.

Here, we report that covalently attached slippery surface coatings can significantly reduce the protein adsorptions on planar PDMS surfaces and in microfluidic channels by using human fibrinogen and albumin as two model serum proteins. Additionally, when interacting with induced neural progenitor cells (iNPCs), these surface coatings are capable of coculturing with iNPCs in a long-term culture. We also confirm that iNPC cultures containing such coatings show a good cell viability compared with the cell-only control group. The optical transparency, low-cost operation, scalable manufacturing, anti-protein adsorption property, and biocompatibility illustrate the potentially wide range of applications ranging from implantable medical devices to wearable sensors.

RESULT AND DISCUSSION

Preparation and characterizations of the slippery surface coating

The slippery surface coatings are prepared by acid-catalyzed polycondensation reaction of dimethyldimethoxysilane due to its simple operation procedures and scalability, thereby enabling the future distribution to the broad end-user community. Briefly, the preparation of slippery surface coatings starts with oxygen plasma treatment of the PDMS surfaces (to generate hydroxyl groups), followed by dip-coating the surface in an isopropanol solution containing dimethyldimethoxysilane and sulfuric acid ~ 30 to 60 seconds and drying at room temperature or in a 75°C oven (Figure 1A). During the drying step, PDMS brushes are rapidly grafted on the surfaces due to the acid-catalyzed hydrolysis and condensation of dimethyldimethoxysilane [33]. As a result, the one end of the formed surface coating (PDMS brush) is covalently attached to the surface through Si-O bond (Figure 1A), while the remaining part of the PDMS brush shows high mobility. To support the formation of the surface coating, XPS spectra of the PDMS surfaces before and after the surface coating are

shown in Figure 1B and S1. From the high-resolution spectra, characteristic peaks, including O1s, C1s, Si2s and Si2p, are observed. For O_2 plasma-treated PDMS surfaces, the hydroxyl groups are generated on the PDMS surface, and thus a high O1s peak is observed. After the surface coating, an increase of carbon/oxygen ratio is observed, indicating the successful grafting of PDMS brushes on oxygen plasma treated surfaces. It should be noted that the XPS measurement of grafted PDMS brushes may be interfered by the underlying substrates. To that end, we further confirm the formation of the surface coating by conducting contact angle measurements. Figure 1C compares the wetting properties of the PDMS surfaces before and after the surface coating presented by the quantitative analysis of static water contact angles measured by using a tensiometer (Data physics OCA). The pristine PDMS surfaces exhibit hydrophobic characteristics with a high-water CA (θ=102.8±4.3°), while O_2 plasma-treated PDMS surfaces present strong affinity with water, leading to low water CAs (θ=7.0±2.9°) due to the formation of the hydroxyl groups (—OH). A significant increase in CA (θ=84.0±4.8°) is observed after the surface coating, indicating the successful grafting of the coating. Importantly, this wettability change before and after the surface coating could be used as a simple visual inspection to examine whether these coatings have been successfully attached on the surface (Figure 1C and S2).

The optical property of the surface coating is critical for implantable optoelectronics, such as optical fibers for optogenetics and photometry.[34] Figure 1D shows the optical transmittance spectra of a surface without coating (control) and with the slippery surface coating. PDMS with the slippery surface coating maintains its superior transparency (~ 90%) in the visible wavelength range. Figure 1E shows optical images of covalently attached slippery surface coating on the top of a white paper with printed words of “slippery surface coatings”, demonstrating the optical transparency of surface coating. The covalently attached PDMS brushes show ‘liquid-like’ properties due to their ultralow glass transition temperature (T_g=−125°C) and excellent slippery properties towards both nonpolar and polar liquid[33]. To test the slippery properties of the surface coating, we measure the mobility of water droplets on PDMS surfaces with and without the slippery coating (Figure 1F and Movies S1 and 2). For PDMS without the surface coating, the water droplet does not slide even the substrates are placed vertically for 120 seconds. In contrast, when a water droplet is placed on the surface with the surface coating, it slides freely from right to left side at a tilting angle of 15°, without any visible wetting trails. Furthermore, the speed-dependent friction coefficients are measured under a constant load force of 1 N (Figure S3). A significant reduction in coefficient of friction is observed for PDMS surfaces after the slippery surface coatings, which is attributed to the formation of covalently attached, highly mobile polydimethylsiloxane (PDMS) brushes on the surface.

Anti-protein adsorption property on planar PDMS surfaces

We evaluate the anti-protein adsorption property of the covalently attached slippery surface coating by using fluorescein conjugated-bovine serum albumin (BSA, FITC conjugate) as a model serum protein. Briefly, PDMS thin films with and without the slippery surface coatings are incubated in 1X phosphate buffered saline (PBS) with a protein concentration of 1 mg/mL at 37 °C for 1 day, 3 days, and 7 days. As shown in the confocal fluorescence microscopy images (green: BSA) in Figure 2A and quantitative average intensity (Figure

2B), many proteins are observed on the surface without the coating as soon as one day after the incubation. In contrast, significantly reduced adsorption (42%-59% reduction) of BSA is observed when the slippery surface coating is applied (Figure 2B and Table S2), mainly because of its slippery 'liquid-like' property of covalently attached PDMS brushes, which can prevent the adsorption of proteins. In the long-term studies, the anti-protein adsorption property of the slippery surface coating is further proved by incubating PDMS thin films with and without the coating for 14 day, 21 days, and 30 days (Figure 2C and Table S2). Mechanical stability is critical for practical applications. To that ends, we investigate the mechanical durability of covalently attached slippery surface coating by stretching at a strain of 5% strain for 10,000 times or stirring in 1X PBS at 500 rpm for three days (Figures S4A and B). The confocal fluorescence microscopy images (Figure S4C) and quantitative average intensity characterizations (Figures S4D-F) suggest that PDMS thin films with the slippery surface coating maintain the capability to significantly reduce the protein adsorptions after mechanical deformations by stretching and stirring (**** $P<0.0001$, *** $P<0.001$). The anti-protein adsorption property of the slippery surface coating was further proved by incubating PDMS with and without the coating in 1 mg/mL fibrinogen (human fibrinogen Alexa Fluor™ 594 conjugates) for 1 day, 3 days, 7 days, 14 days, 21 days, and 30 days (Figure 2D-F and Table S2).

Anti-protein adsorption property on 3D PDMS microfluidic channels

Inspired by the significant reduction of protein adsorptions with the slippery surface coating on planar PDMS surfaces, we then wonder whether such coatings could be adapted to 3D microfluidic channels as microfluidic channels have multiple applications ranging from implantable neural probes for drug delivery to platforms for organs-on-chips.[35] To answer this question, we studied the anti-protein adsorption property on 3D PDMS microfluidic channels. Figure 3A shows the schematic illustrates of the setup, including a syringe pump, a microsyringe that contains protein-rich solutions, and 3D microfluidic channels with liquid-like surface coatings. Figure 3B shows an optical image of a PDMS device with multiple 3D microfluidic channels. The protein-rich solution (1mg/mL human fibrinogen or BSA) is infused through microfluidic channels with a flow rate of 1μL/min by using a syringe pump. 3D mapping images which incorporate the whole depths of microfluidic channels from bottom to top layers as a function of time are shown in Figure 3C. Fibrinogens (red fluorescence) are observed in microfluidic channels without the surface coatings. The fluorescence intensity increases significantly from 0 min to 5 min and reaches to the plateau from 5 min to 20 min. In contrast, microfluidic channels with the slippery coating show the reduced fluorescence signals (Figure 3C). Quantitative analysis of the fluorescence intensity using ImageJ further confirm the reduced protein adsorptions (55%-79% reduction for BSA and 44% to 57% reduction for fibrinogen) for 3D microfluidic channels with the surface coatings (Figures 3D and E, and Table S3) mainly because highly mobile PDMS brushes attached on the channel surfaces prevent the protein adsorptions. To further evaluate the effective cleaning of the surface coatings on the microfluidic channels, we also performed related experiments using DI water to flush through the microfluidic channel after emptying the protein solution. Figure S5 shows the changes in fluorescence intensity as a function of time for effective cleaning. With slippery surface coated microfluidic channels, the proteins were easily and quickly removed, resulting in

a significant decrease in intensity signal as soon as 1 minute. In contrast, with uncoated microfluidic channels, the protein remained attached to the surface of the microfluidic channels and a much smaller decrease in the fluorescence intensity was observed. Overall, this study suggests the effective cleaning of 3D PDMS microfluidic channels using slippery surface coatings.

Cell metabolic activity determined by MTT assay

Biocompatibility is a key consideration for the *in vivo* applications of the developed surface coating, which determines how long and how well they are capable of sustaining their functionality in the physiological environment. Human cortical spheroid or organoid models have emerged as a promising platform for neurotoxicity, drug screening, and disease modeling studies.[36, 37] Our previous study has investigated the interactions of cortical spheroids with various biomaterials, including nanoparticles and microplastics.[38] The timeline of cortical spheroid formation and iNPC development from hiPSCs was shown in Figure 4A. MTT activity shows cell viability and metabolic activity observed over 1, 3, 5, and 7 days for bare PDMS and PDMS with the slippery surface coating in the coculture systems in comparison with the cell-only group (Figure 4B). With the culture time increase, the activity of iNPCs increased and reached a plateau. iNPC morphology shows the occurrence of neural network after 10-day replating and coculturing with PDMS and with slippery surface coatings, respectively (Figure 4C). These results indicate that the biocompatibility of the slippery surface coatings with the iNPCs is comparable to the cell-only group.

Cell viability determined by live and dead flow cytometry assay

For the biocompatibility of slippery surface coatings with iNPCs of the cortical spheroids, there are two different types of experiments conducted: a short-term 7-day coculture and a long-term 21-day co-culture. The cell viabilities are measured by live/dead assay quantified by flow cytometry. The short-term culture data are shown in Figure 4D, 4E, and 4F, and the long-term culture data are shown in Figure 4G, 4H, and 4I. For short-term culture, the live cells in the PDMS with slippery surface coatings culture were 74.9%, slightly lower than 84.7% of the cell-only group (control) and 87.4% of the PDMS group. For the long-term culture, the PDMS with slippery surface coatings has 83.9% of live cells, comparable to the cell-only group (88.6%) and slightly higher than the PDMS group (77.8%). These results further support the biocompatibility of the slippery surface coatings.

CONCLUSION

We demonstrate that the liquid-like slippery coating significantly reduces the adsorptions of pro-inflammatory serum proteins, human fibrinogen and albumin, on planar PDMS surfaces and in 3D microfluidic channels. The preparation of the surface coating relies on scalable and simple dip-coating methods. UV-vis spectra reveal the optical transparency of the surface coating, thereby enabling potential applications in optoelectronic devices. Additionally, MTT data show that the surface coating has good biocompatibility as PDMS and cell-only coculture systems with the iNPCs. In addition, both short-term (7 days) and long-term (21 days) studies by live and dead assay shows good cell viability of the prepared

surface coatings. These results lay a foundation for the future applications of slippery surface coatings to reduce protein adsorptions for basic biomedical research and clinical medicine.

EXPERIMENTAL SECTION

Materials.

2-Propanol (≥99.5%), Sulfuric acid (95%-98%), Dimethyldimethoxysilane (95%), Agarose, Dulbecco's Phosphate Buffered Saline with $MgCl_2$ and $CaCl_2$, 100 mL Sodium bicarbonate solution (7.5%), Poly (methyl methacrylate) (PMMA), Accutase® solution, LDN193189 (a bone morphogenetic protein inhibitor), SB431542 (a transforming growth factor inhibitor), 3-(4,5-Dimethyl-2-thiazolyl)-2,5-diphenyl-2H-tetrazolium bromide (MTT), Retinoic acid 98% (RA) were purchased from Sigma-Aldrich (St. Louis, MO). Polydimethylsiloxane (PDMS, Dow SYLGARD™ 184) was purchased from Ellsworth Adhesives (Germantown, WI). Bovine serum albumin (BSA, FITC conjugate), Fibrinogen from human plasma (Alexa Fluor™ 594 Conjugate), minimum essential medium-alpha(α-MEM), Dulbecco's Modified Eagle Medium (DMEM/F12) were received from Thermo Fisher Scientific (Waltham, MA). mTeSRTM 1 medium (20 mL mTeSRTM 1 basal and 5 mL mTeSRTM 1 5X supplement) was purchased from STEMCELL Technology, Inc. (Cambridge, MA). B-27 serum-free supplement, Fibroblast growth factor-2 (FGF2), and Penicillin/Streptomycin were purchased from Life Technologies (Carlsbad, CA). Fetal bovine serum (FBS) was purchased from Atlanta Biologicals (Lawrenceville, GA). Y27632 (a Rho-associated kinase inhibitor) was purchased from iXCells, Biotechnologies, (San Diego, CA). Growth factor reduced Matrigel, 150 mm tissue culture petri dish, 24-well and 96-well ultra-low attachment, 6-well, 24-well, and 96-well tissue culture plates were purchased from Corning (Corning, NY). Silicon wafers were bought from University Wafers. Ultrapure water applied in all the washing steps is run by Milli-Q® Type 1 system.

Preparation and characterizations of slippery surface coatings on PDMS surfaces.

PDMS thin films (thickness: ~40 μm) were prepared by spin coating silicone elastomers (elastomer/curing agent ratio, 10:1; Sylgard 184, Dow Corning) at 2000 rpm for 30 s on a poly(methyl methacrylate) (PMMA)-coated silicon wafer. The prepared PDMS thin films were then cured either in a 75°C oven for one hour and treated with oxygen plasma (Harrick Plasma Inc.). In parallel, 2-propanol, dimenthyldimethoxysilane, and sulfuric acid were added to a 20 mL glass vial to prepare the reaction solution; the volume ratio of 2-propanol to dimenthyldimenthoxysilane to sulfuric acid was kept at 100:10:1. Next, the oxygen plasma treated PDMS thin films were dip-coated in the reactive solution for ~ 30-60 seconds and then dried at room temperature or at 75°C in the oven.

UV-vis spectra and transparency tests.

The transparency of PDMS thin films with and without slippery surface coatings was measured by using a V-770 UV-Visible/NIR Spectrophotometer (Easton, MD) under the wavelength range from 100 nm to 900 nm.

XPS measurements.

Thermo Scientific K-Alpha X-ray photoelectron spectrometer (XPS) was used to characterize PDMS thin films with oxygen plasma treatments (n=3) and three samples functionalized with the slippery surface coating.

Characterization of anti-protein adsorption property on planar PDMS surfaces.

A total of 5 mg BSA powder (FITC conjugate) was dissolved in the Dulbecco's Phosphate Buffered Saline to prepare 1mg/mL BSA-rich solution. Similarly, 5mg human fibrinogen powder (Alexa Fluor™ 594 Conjugate) was dissolved in sodium bicarbonate solution to make solution containing fibrinogen. The PDMS thin films treated with and without surface coatings on the silicon wafer were incubated in glass vials containing the BSA or human fibrinogen solution at 37°C for 1 day, 3 days, 7 days, 14 days, 21 days, and 30 days, respectively. Nikon A1R HD Confocal Microscope was used to capture high-resolution confocal images at excitation wavelengths of 488 nm (for BSA) and 558 nm (for fibrinogen).

Characterization of anti-protein adsorption property on 3D PDMS microfluidic channels.

3D PDMS microfluidic channels (cross section width: 200 μm; height: 50 μm) were prepared by using standard soft lithography and molding process on a SU-8 mold. The abovementioned reactive solution was pumped into oxygen plasma-treated channels 10 min to form the slippery surface coatings. The functionalized 3D microfluidic channels were then rinsed with DI water several times, and dried in a 75°C oven. The characterization of anti-protein adsorption property started with infusing a protein-rich solution (1 mg/mL BSA in 1X PBS or 1 mg/mL fibrinogen in sodium bicarbonate solution) with a flow rate at 1 μL/min into microfluidic channels which connected with a plastic tube. Confocal images were captured at 0 min, 5 min, 10 min, 15 min and 20 min. Z-stack scanning (150 μm in total, with each step of 10 μm) was performed at a scanning speed of 1.56 s per step. Repeated experiment was performed at least 3 three times for each group.

Human-induced pluripotent stem cell (hiPSC) culture.

The culture of hiPSCs was performed following our previous publications.[39, 40] Human iPSK3 cells were derived from human foreskin fibroblast transfected with plasmid DNA encoding reprogramming factors OCT4, NANOG, SOX2, and LIN28. Briefly, the 6-well tissue culture plate was coated with Matrigel (1:30 dilution in DMEM/F12) and incubated at 37 °C. The cells were dissociated by Accutase for 5-10 min at 37 °C. Then, 1.5×10^6 cells were seeded onto the Matrigel-coated 6-well plate in the presence of 10 μM Y-27632 in mTESR medium. The medium was changed every day, and the cells were passaged once a week.

Cortical spheroid differentiation from hiPSCs.

The cortical spheroid differentiation was performed as shown in our previous publications[41, 42]. Briefly, the dissociated hiPSCs were seeded into the ultra-low attachment 24-well plate at 3×10^5 cells per well in the differentiation medium (DMEM/F12 + 2% B-27) and 10 μM Y-27632. After 24h incubation, the culture medium was changed to

DMEM/F12/2% B27 with 10 μM SB431542 (a potent and selective inhibitor of the transforming growth factor-β pathway) and 100 nM LDN193189 (a potent inhibitor of the bone morphogenetic pathway). The medium was changed every other day. On day 8, the medium was changed to DMEM/F12/2% B-27 with 10 ng/mL FGF2 and 5 μM RA. This culture was maintained for another 8 days. The formed cortical spheroids were then replated onto Matrigel-coated surfaces until the neural network was established (around 10 days). This cell population was referred to as hiPSC-derived neural progenitor cells (iNPCs).

MTT assay for biocompatibility study.

For a short-term biocompatibility study, the day-16 iNPCs were replated to the 96-well tissue culture plate containing PDMS with the slippery surface coating in neural differentiation medium. There are three groups used for comparison of the MTT activity. PDMS and cell-only conditions were tested as the control groups. The cells were incubated with 5 mg/mL MTT solution at days 1, 3, 5, and 7 for 2-4 hours. Then, the formazan crystals were centrifuged and hydrolyzed by dimethyl sulfoxide (DMSO) (Sigma). Afterward, the pink solution was read at 570 nm by the microplate reader (BioRad Laboratories, Hercules, CA).

Live/Dead assay analyzed by two-color flow cytometry.

The cell viability of the PDMS with or without coatings in the coculture system was determined using the Live/Dead™ staining kit (Molecular Probes) according to the manufacturer's protocol. For the short-term biocompatibility study, after 7-day culture, the replated iNPCs were dissociated by the Accutase for 40 min to make single-cell solutions. For the long-term biocompatibility study with neural cells, after 21-day coculture, the iNPCs were dissociated by Accutase for 40 min to make single-cell solutions. Then, 50 μM calcein AM and 2 mM ethidium homodimer-1 were added to the cell suspensions. The cells were incubated for 15–20 minutes at room temperature, protected from light. The stained cells were acquired by BD FACSCanto II flow cytometer using 488 nm excitation and measuring green fluorescence emission for calcein (i.e., 530/30 bandpass) and red fluorescence emission for ethidium homodimer-1 (i.e., 610/20 bandpass) within 1-2 hours. The acquired events were analyzed with proper color compensation against negative controls using FlowJo software.

Statistical Analysis.

Student’s t-test was used for the statistical analysis of protein adsorption experiments. A one-way analysis of variance (ANOVA) was conducted to compare the cell viabilities by MTT assay. All groups were compared with each other with Tukey's multiple comparisons test. Image J software was utilized to calculate and fully interpret the intensity of fluorescence signals.

Supplementary Material

Refer to Web version on PubMed Central for supplementary material.

Acknowledgement

This work is supported by the University of Connecticut start-up fund, NIH RF1NS118287, and R01MH128721. The content is solely the responsibility of the authors and does not necessarily represent the official views of the National Institutes of Health. Partial support was received from National Science Foundation (CBET 1917618). The authors would also thank for the support by Florida State University Flow Cytometry Core facility.

References:

(1). Teo AJT; Mishra A; Park I; Kim YJ; Park WT; Yoon YJ Polymeric Biomaterials for Medical Implants and Devices. ACS Biomater Sci Eng 2016, 2 (4), 454–472. DOI: 10.1021/acsbiomaterials.5b00429. [PubMed: 33465850]

(2). Doloff JC; Veiseh O; de Mezerville R; Sforza M; Perry TA; Haupt J; Jamiel M; Chambers C; Nash A; Aghlara-Fotovat S; et al. The Surface Topography of Silicone Breast Implants Mediates the Foreign Body Response in Mice, Rabbits and Humans. Nat Biomed Eng 2021, 5 (10), 1115–1130. DOI: 10.1038/s41551-021-00739-4. [PubMed: 34155355]

(3). McLaughlin K, J. B, Mactier R, Porteus C Long-Term Vascular Access for Hemodialysis Using Silicon Dual-Lumen Catheters with Guidewire Replacement of Catheters for Technique Salvage. Am J Kidney Dis 1997, 29 (4), 553–559. DOI: 10.1016/s0272-6386(97)90337-1. [PubMed: 9100044]

(4). Lloyd AW, F. R, Denyer SP. Ocular Biomaterials and Implants. Biomaterials 2001, 22 (8), 769–785. DOI: 10.1016/s0142-9612(00)00237-4. [PubMed: 11246945]

(5). Zhu Y; Li S; Li J; Falcone N; Cui Q; Shah S; Hartel MC; Yu N; Young P; de Barros NR; et al. Lab-on-a-Contact Lens: Recent Advances and Future Opportunities in Diagnostics and Therapeutics. Adv Mater 2022, 34 (24), e2108389. DOI: 10.1002/adma.202108389. [PubMed: 35130584]

(6). Filippi M; Buchner T; Yasa O; Weirich S; Katzschmann RK Microfluidic Tissue Engineering and Bio-Actuation. Adv Mater 2022, 34 (23), e2108427. DOI: 10.1002/adma.202108427. [PubMed: 35194852]

(7). Koh A; Kang D; Xue Y; Lee S; Pielak RM; Kim J; Hwang T; Min S; Banks A; Bastien P; et al. A Soft, Wearable Microfluidic Device for the Capture, Storage, and Colorimetric Sensing of Sweat. Sci Transl Med 2016, 8 (366), 366ra165. DOI: 10.1126/scitranslmed.aaf2593.

(8). Zhang Y; Guo H; Kim SB; Wu Y; Ostojich D; Park SH; Wang X; Weng Z; Li R; Bandodkar AJ; et al. Passive Sweat Collection and Colorimetric Analysis of Biomarkers Relevant to Kidney Disorders Using a Soft Microfluidic System. Lab Chip 2019, 19 (9), 1545–1555. DOI: 10.1039/c9lc00103d. [PubMed: 30912557]

(9). Huang X; Li J; Liu Y; Wong T; Su J; Yao K; Zhou J; Huang Y; Li H; Li D; et al. Epidermal Self-Powered Sweat Sensors for Glucose and Lactate Monitoring. Bio-Des Manuf 2021, 5 (1), 201–209. DOI: 10.1007/s42242-021-00156-1.

(10). Zhang Y; Mickle AD; Gutruf P; McIlvried LA; Guo H; Wu Y; Golden JP; Xue Y; Grajales-Reyes JG; Wang X; et al. Battery-Free, Fully Implantable Optofluidic Cuff System for Wireless Optogenetic and Pharmacological Neuromodulation of Peripheral Nerves. Sci Adv 2019, 5 (7), eaaw5296. DOI: doi:10.1126/sciadv.aaw5296. [PubMed: 31281895]

(11). Zhang Y; Castro DC; Han Y; Wu Y; Guo H; Weng Z; Xue Y; Ausra J; Wang X; Li R; et al. Battery-Free, Lightweight, Injectable Microsystem for in Vivo Wireless Pharmacology and Optogenetics. Proc Natl Acad Sci USA 2019, 116 (43), 21427–21437. DOI: 10.1073/pnas.1909850116. [PubMed: 31601737]

(12). Wu G; Heck I; Zhang N; Phaup G; Zhang X; Wu Y; Stalla DE; Weng Z; Sun H; Li H; et al. Wireless, Battery-Free Push-Pull Microsystem for Membrane-Free Neurochemical Sampling in Freely Moving Animals. Sci Adv 2022, 8 (8), eabn2277. DOI: doi:10.1126/sciadv.abn2277. [PubMed: 35196090]

(13). Kozai TD; Jaquins-Gerstl AS; Vazquez AL; Michael AC; Cui XT Brain Tissue Responses to Neural Implants Impact Signal Sensitivity and Intervention Strategies. ACS Chem Neurosci 2015, 6 (1), 48–67. DOI: 10.1021/cn500256e. [PubMed: 25546652]

(14). Eles JR; Vazquez AL; Kozai TDY; Cui XT Meningeal Inflammatory Response and Fibrous Tissue Remodeling around Intracortical Implants: An in Vivo Two-Photon Imaging Study. Biomaterials 2019, 195, 111–123. DOI: 10.1016/j.biomaterials.2018.12.031. [PubMed: 30634095]

(15). Maan AMC; Hofman AH; Vos WM; Kamperman M Recent Developments and Practical Feasibility of Polymer-Based Antifouling Coatings. Adv Funct Mater 2020, 30 (32), 1–30. DOI: 10.1002/adfm.202000936.

(16). McVerry B; Polasko A; Rao E; Haghniaz R; Chen D; He N; Ramos P; Hayashi J; Curson P; Wu CY; et al. A Readily Scalable, Clinically Demonstrated, Antibiofouling Zwitterionic Surface Treatment for Implantable Medical Devices. Adv Mater 2022, 34 (20), e2200254. DOI: 10.1002/adma.202200254. [PubMed: 35315553]

(17). Bjugstad KB; Redmond DE Jr.; Lampe KJ; Kern DS; Sladek JR Jr.; Mahoney MJ Biocompatibility of Peg-Based Hydrogels in Primate Brain. Cell Transplant 2008, 17 (4), 409–415.. [PubMed: 18522243]

(18). Lynn AD; Blakney AK; Kyriakides TR; Bryant SJ Temporal Progression of the Host Response to Implanted Poly(Ethylene Glycol)-Based Hydrogels. J Biomed Mater Res A 2011, 96 (4), 621–631. DOI: 10.1002/jbm.a.33015. [PubMed: 21268236]

(19). Browning MB; Cereceres SN; Luong PT; Cosgriff-Hernandez EM Determination of the in Vivo Degradation Mechanism of Pegda Hydrogels. J Biomed Mater Res A 2014, 102 (12), 4244–4251. DOI: 10.1002/jbm.a.35096. [PubMed: 24464985]

(20). Golabchi A; Wu B; Cao B; Bettinger CJ; Cui XT Zwitterionic Polymer/Polydopamine Coating Reduce Acute Inflammatory Tissue Responses to Neural Implants. Biomaterials 2019, 225, 119519. DOI: 10.1016/j.biomaterials.2019.119519. [PubMed: 31600673]

(21). Nandanan Erathodiyil H-MC, Hong Wu, Ying Jackie Y.. Zwitterionic Polymers and Hydrogels for Antibiofouling Applications in Implantable Devices. Mater Today 2020, 38, 84–98. DOI: 10.1016/j.mattod.2020.03.024.

(22). Yang Q; Wu B; Eles JR; Vazquez AL; Kozai TDY; Cui XT Zwitterionic Polymer Coating Suppresses Microglial Encapsulation to Neural Implants in Vitro and in Vivo. Adv Biosyst 2020, 4 (6), e1900287. DOI: 10.1002/adbi.201900287. [PubMed: 32363792]

(23). Chan D; Chien J-C; Axpe E; Blankemeier L; Baker SW; Swaminathan S; Piunova VA; Zubarev DY; Maikawa CL; Grosskopf AK; Mann JL; Soh HT; Appel EA Combinatorial Polyacrylamide Hydrogels for Preventing Biofouling on Implantable Biosensors. Adv. Mater 2022, 34, 2109764 .

(24). Leslie DC; Waterhouse A; Berthet JB; Valentin TM; Watters AL; Jain A; Kim P; Hatton BD; Nedder A; Donovan K; et al. A Bioinspired Omniphobic Surface Coating on Medical Devices Prevents Thrombosis and Biofouling. Nat Biotechnol 2014, 32 (11), 1134–1140. DOI: 10.1038/nbt.3020. [PubMed: 25306244]

(25). Sun H; Li R; Li H; Weng Z; Wu G; Kerns P; Suib S; Wang X; Zhang Y Bioinspired Oil-Infused Slippery Surfaces with Water and Ion Barrier Properties. ACS Appl Mater Interfaces 2021, 13 (28), 33464–33476. DOI: 10.1021/acsami.1c06632. [PubMed: 34241991]

(26). Han K; Wang Z; Heng L; Jiang L Photothermal Slippery Surfaces Towards Spatial Droplet Manipulation. J Mater Chem A 2021, 9 (31), 16974–16981. DOI: 10.1039/d1ta04243b.

(27). Guo P; Wang Z; Heng L; Zhang Y; Wang X; Jiang L Magnetocontrollable Droplet and Bubble Manipulation on a Stable Amphibious Slippery Gel Surface. Adv Funct Mater 2019, 29 (11), 1–10. DOI: 10.1002/adfm.201808717.

(28). Lee Y; Shin H; Lee D; Choi S; Cho IJ; Seo J A Lubricated Nonimmunogenic Neural Probe for Acute Insertion Trauma Minimization and Long-Term Signal Recording. Adv Sci 2021, 8 (15), e2100231. DOI: 10.1002/advs.202100231.

(29). Soumyadip Sett XY, George Barac, Bolton Leslie W., and Nenad Miljkovic. Lubricant-Infused Surfaces for Low-Surface-Tension Fluids: Promise Versus Reality. ACS Appl Mater Interfaces 2017, 9 (41), 36400–36408. DOI: 10.1021/acsami.7b10756. [PubMed: 28950702]

(30). Wang Z; Xu Q; Wang L; Heng L; Jiang L Temperature-Induced Switchable Interfacial Interactions on Slippery Surfaces for Controllable Liquid Manipulation. J Mater Chem A 2019, 7 (31), 18510–18518. DOI: 10.1039/c9ta05164c.

(31). Wang X; Wang Z; Heng L; Jiang L Stable Omniphobic Anisotropic Covalently Grafted Slippery Surfaces for Directional Transportation of Drops and Bubbles. Adv Funct Mater 2019, 30 (1), 1–10. DOI: 10.1002/adfm.201902686.

(32). Wu Q; Yang C; Su C; Zhong L; Zhou L; Hang T; Lin H; Chen W; Li L; Xie X Slippery Liquid-Attached Surface for Robust Biofouling Resistance. ACS Biomater Sci Eng 2020, 6 (1), 358–366. DOI: 10.1021/acsbiomaterials.9b01323. [PubMed: 33463210]

(33). Wang L; McCarthy TJ Covalently Attached Liquids: Instant Omniphobic Surfaces with Unprecedented Repellency. Angew Chem Int Ed 2016, 55 (1), 244–248. DOI: 10.1002/anie.201509385.

(34). Lu L; Gutruf P; Xia L; Bhatti DL; Wang X; Vazquez-Guardado A; Ning X; Shen X; Sang T; Ma R; et al. Wireless Optoelectronic Photometers for Monitoring Neuronal Dynamics in the Deep Brain. Proc Natl Acad Sci USA 2018, 115 (7), E1374–E1383. DOI: 10.1073/pnas.1718721115. [PubMed: 29378934]

(35). Shakeri A; Khan S; Didar TF Conventional and Emerging Strategies for the Fabrication and Functionalization of Pdms-Based Microfluidic Devices. Lab Chip 2021, 21 (16), 3053–3075. DOI: 10.1039/d1lc00288k. [PubMed: 34286800]

(36). Tan HY; Cho H; Lee LP Human Mini-Brain Models. Nat Biomed Eng 2021, 5 (1), 11–25. DOI: 10.1038/s41551-020-00643-3. [PubMed: 33318650]

(37). Garreta E, Kamm RD, Chuva de Sousa Lopes SM et al. Rethinking Organoid Technology through Bioengineering. Nat Mater 2020, 20, 145–155. DOI: 10.1038/s41563-020-00804-4. [PubMed: 33199860]

(38). Marzano M; Bou-Dargham MJ; Cone AS; York S; Helsper S; Grant SC; Meckes DG Jr.; Sang QA; Li Y Biogenesis of Extracellular Vesicles Produced from Human-Stem-Cell-Derived Cortical Spheroids Exposed to Iron Oxides. ACS Biomater Sci Eng 2021, 7 (3), 1111–1122. DOI: 10.1021/acsbiomaterials.0c01286. [PubMed: 33525864]

(39). Yan Y BJ, Xia J Guan J Zhou Y Li Y Neural Patterning of Human Induced Pluripotent Stem Cells in 3-D Cultures for Studying Biomolecule-Directed Differential Cellular Responses. Acta Biomater 2016, 42, 114–126. DOI: 10.1016/j.actbio.2016.06.027. [PubMed: 27345135]

(40). Yan Y; Song L; Madinya J; Ma T; Li Y Derivation of Cortical Spheroids from Human Induced Pluripotent Stem Cells in a Suspension Bioreactor. Tissue Eng Part A 2018, 24 (5-6), 418–431. DOI: 10.1089/ten.TEA.2016.0400. [PubMed: 28825364]

(41). Song L; Yuan X; Jones Z; Vied C; Miao Y; Marzano M; Hua T; Sang QA; Guan J; Ma T; et al. Functionalization of Brain Region-Specific Spheroids with Isogenic Microglia-Like Cells. Sci Rep 2019, 9 (1), 11055. DOI: 10.1038/s41598-019-47444-6. [PubMed: 31363137]

(42). Song L; Yuan X; Jones Z; Griffin K; Zhou Y; Ma T; Li Y Assembly of Human Stem Cell-Derived Cortical Spheroids and Vascular Spheroids to Model 3-D Brain-Like Tissues. Sci Rep 2019, 9 (1), 5977. DOI: 10.1038/s41598-019-42439-9. [PubMed: 30979929]

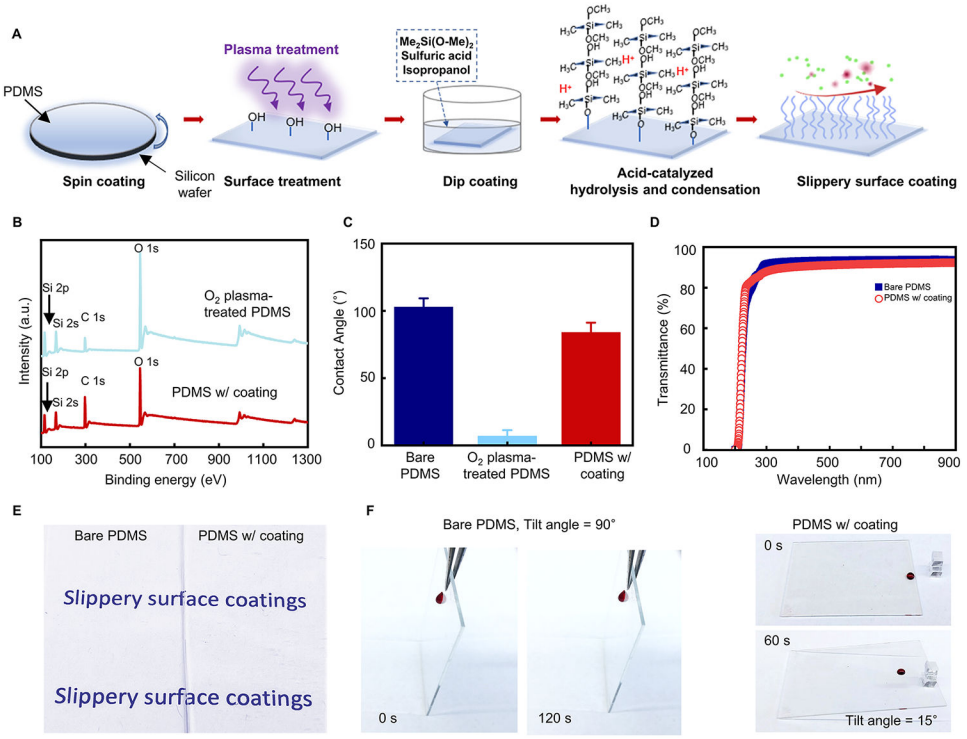

Figure 1. Preparation and characterization of the slippery surface coating.

(**A**) Schematic illustration for the preparation of the surface coating based on acid-catalyzed polycondensation reaction of dimethyldimethoxysilane. (**B**) XPS spectra of oxygen plasma-treated PDMS with and without the surface coating. (**C**) Static water contact angles on PDMS surfaces, oxygen plasma-treated PDMS surfaces, and surfaces with coatings. n=5. (**D**) UV-Vis spectra of PDMS thin films with and without the slippery surface coating. (**E**) White paper with printed words “slippery surface coatings” covered by PDMS thin films with and without the surface coating. (**F**) The mobility of water droplets (with red dye) on PDMS surfaces with and without the coating.

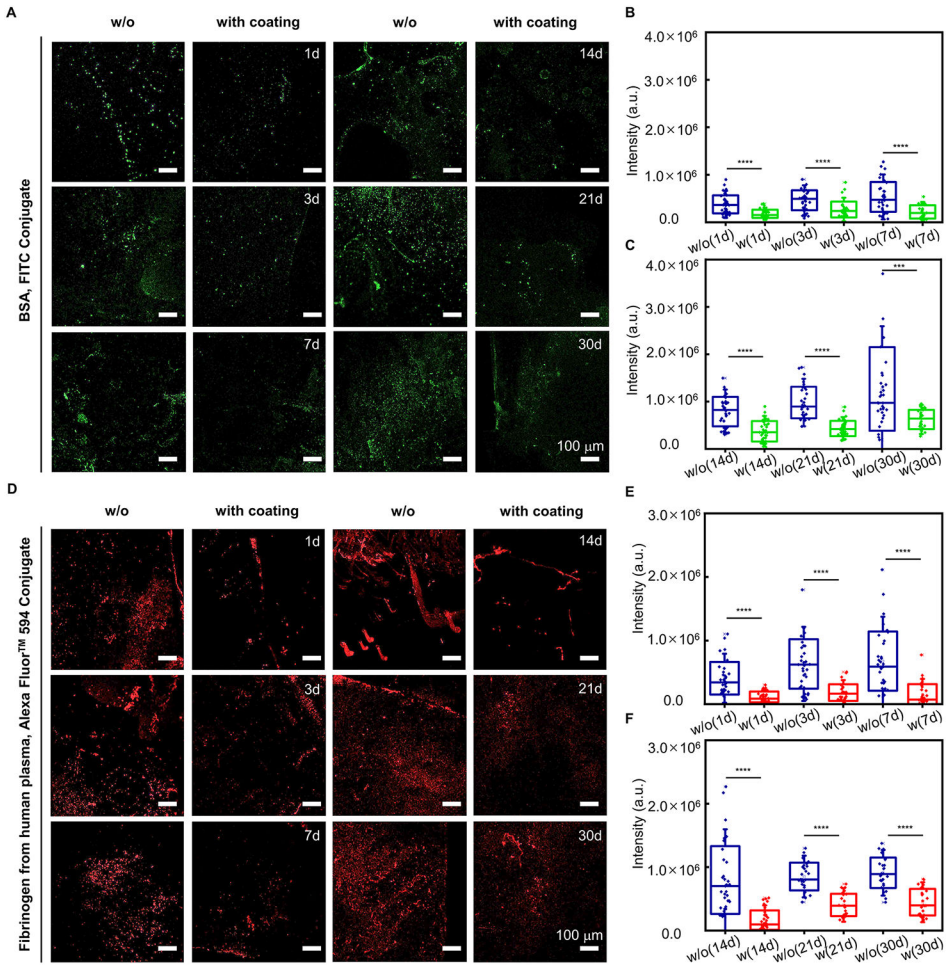

Figure 2. Anti-protein adsorption property of planar PDMS surfaces with and without the slippery coating.

(**A**) Representative confocal fluorescence microscopy images and (**B, C**) quantitative analysis of the average intensity of planar PDMS thin films without (control) and with slippery coating incubated in 1 mg/mL BSA-FITC conjugates(green) for 1,3,7,14,21 and 30 days. **** P<0.0001, *** P<0.001. (**D**) Representative confocal fluorescence microscopy images and (**E, F**) quantitative analysis of the average intensity of planar PDMS surfaces with and without slippery surface coatings incubated in 1 mg/mL fibrinogen Alexa Fluor™ 594 conjugates for different days. **** P<0.0001. Data are displayed with mean values ± standard deviation. Statistical significance is evaluated by Student's t-tests.

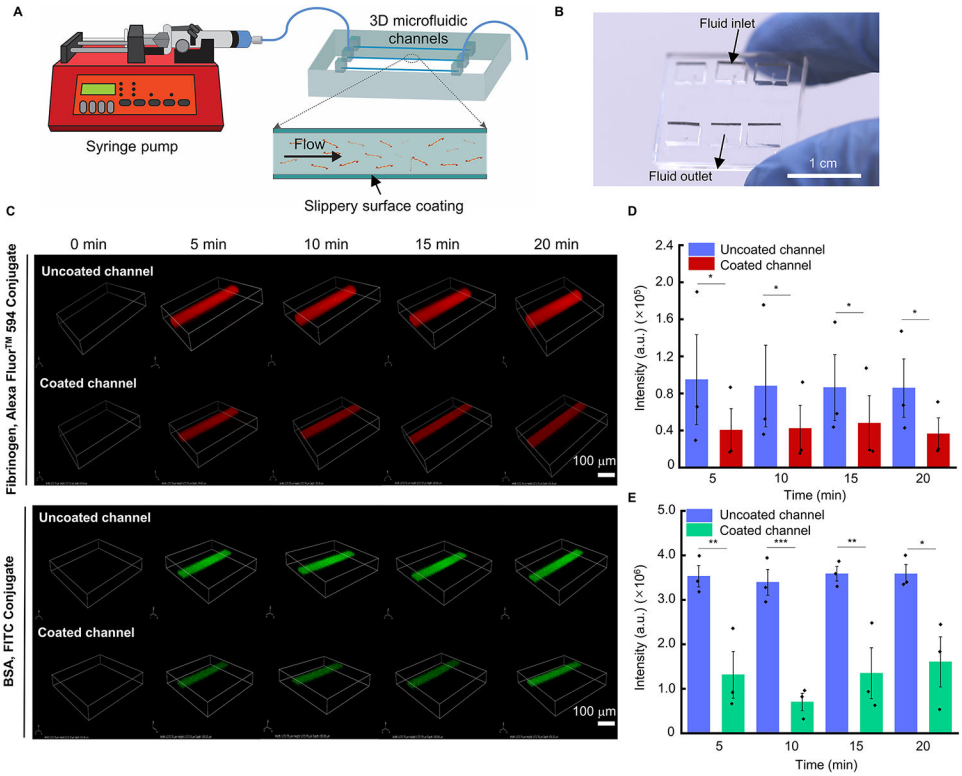

Figure 3. Anti-protein adsorption property on 3D PDMS microfluidic channels.

(**A**) Schematic illustration of the setup to evaluate the anti-protein adsorption property in PDMS microfluidic channels. (**B**) Optical image of a representative microfluidic device. (**C**) 3D mapping confocal fluorescence images of 3D microfluidic channels with and without slippery surface coatings infused with fibrinogen (red) and BSA-FITC (green) solutions. (**D, E**) Quantitative analysis of average fluorescence intensity as a function of time for microfluidic channels with and without surface coatings. n=3. Data are displayed with mean values ± standard deviation. **P*<0.05, ** *P*<0.01, *** *P*<0.001. Statistical analysis is performed by Student's t-tests.

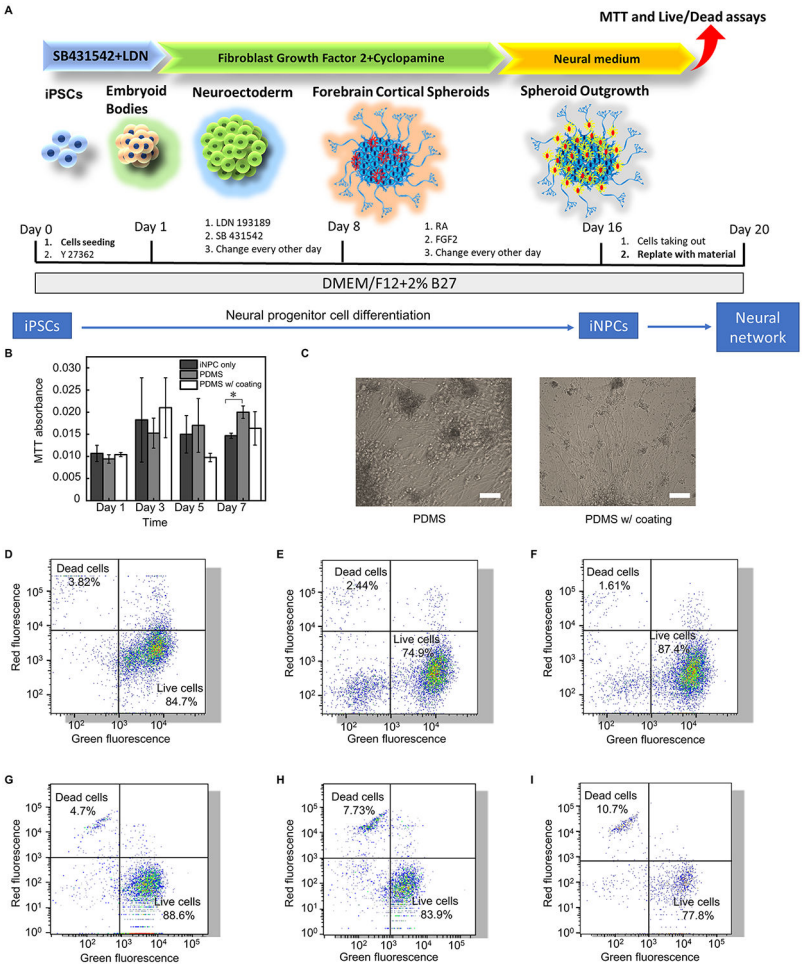

Figure 4. Biocompatibility test of the slippery surface coating coculture system with iNPCs.

(**A**) Timeline of cortical spheroid and iNPC derivation from hiPSC and the coculture. (**B**) MTT activity of iNPCs cocultured with biofilm. Statical analysis was conducted by one-way analysis of variance (ANOVA) with Tukey's test; (n=4). (**C**) iNPC morphology showed the occurrence of the neural network after 10-day replated and coculture with bare PDMS and PDMS with the slippery surface coating, respectively. Scale bar = 100 μm. (**D, E, F**) Flow cytometry plots of live/dead assay for short-term culture (7 days) with cell only, PDMS with coating, and bare PDMS, respectively. (**G, H, I**) Flow cytometry plots of live/dead assay for long-term culture (21 days) with cell only, PDMS with coating, and bare PDMS, respectively. Green fluorescence indicates the live cell population and red fluorescence indicates the dead cell population.